







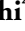







From tree to plot: investigating stem CO₂ efflux and its drivers along a logging gradient in Sabah, Malaysian Borneo

Maria B. Mills¹ , Sabine Both² , Palasiah Jotan³ , Walter Huaraca Huasco⁴ , Rudi Cruz^{5,6} , Milenka M. Pillco⁶ , David F. R. P. Burslem⁷ , Colin Maycock⁸ , Yadvinder Malhi⁴ , Robert M. Ewers⁹, Juan Carlos Berrio¹ , Jörg Kaduk¹ , Susan Page¹ , Rolando Robert¹⁰, Yit A. Teh¹¹  and Terhi Riutta^{4,9,12} 

¹School of Geography, Geology and the Environment, University of Leicester, Leicester, LE1 7RH, UK; ²School of Environmental and Rural Science, University of New England, Armidale, NSW, 2351, Australia; ³Faculty of Forestry and Wood Sciences, Czech University of Life Sciences, Prague, 165 00, Czech Republic; ⁴School of Geography and the Environment, Environmental Change Institute, University of Oxford, Oxford, OX1 3QY, UK; ⁵Instituto de Ciencias de la Naturaleza, Territorio y Energías Renovables, Pontificia Universidad Católica del Perú, Lima, 15088, Peru; ⁶Universidad Nacional de San Antonio Abad del Cusco, Cusco, 08003, Peru; ⁷School of Biological Sciences, University of Aberdeen, Aberdeen, AB24 3UU, UK; ⁸University Malaysia Sabah, Kota Kinabalu, 88400, Malaysia; ⁹Department of Life Science, Imperial College London, London, SL5 7PY, UK; ¹⁰Sabah Forestry Department, Forest Research Centre, Sandakan, Sabah, 90715, Malaysia; ¹¹School of Natural and Environmental Sciences, Newcastle University, Newcastle, NE1 4LB, UK; ¹²UK Centre for Ecology and Hydrology (UK CEH), Lancaster, OX10 8BB, UK

Summary

Author for correspondence:
Maria B. Mills
Email: mbmills96@outlook.com

Received: 14 June 2024
Accepted: 18 July 2024

New Phytologist (2024)
doi: 10.1111/nph.20043

Key words: carbon fluxes, degraded forest, land-use, logging, stem respiration, tropical forest.

- Stem respiration constitutes a substantial proportion of autotrophic respiration in forested ecosystems, but its drivers across different spatial scales and land-use gradients remain poorly understood. This study quantifies and examines the impact of logging disturbance on stem CO₂ efflux (EA) in Malaysian Borneo.
- EA was quantified at tree- and stand-level in nine 1-ha plots over a logging gradient from heavily logged to old-growth using the static chamber method.
- Tree-level results showed higher EA per unit stem area in logged vs old-growth plots (37.0 ± 1.1 vs 26.92 ± 1.14 g C m⁻² month⁻¹). However, at stand-level, there was no difference in EA between logged and old-growth plots (6.7 ± 1.1 vs 6.0 ± 0.7 Mg C ha⁻¹ yr⁻¹) due to greater stem surface area in old-growth plots. Allocation to growth respiration and carbon use efficiency was significantly higher in logged plots. Variation in EA at both tree- and stand-level was driven by tree size, growth and differences in investment strategies between the forest types.
- These results reflect different resource allocation strategies and priorities, with a priority for growth in response to increased light availability in logged plots, while old-growth plots prioritise maintenance and cell structure.

Introduction

Tropical forests play a major role in the global carbon balance, capturing *c.* 72 Pg C from the atmosphere each year, which is *c.* 60% of the global photosynthesis (Beer *et al.*, 2010), but they also release a similar amount back into the atmosphere through respiratory processes in the ecosystem by plants, animals, microorganisms and fungi (Malhi, 2012; Sitch *et al.*, 2015). Understanding the balance between carbon uptake and release in tropical forests requires knowledge of all components of the carbon budget. Respiration from tree stems remains one of the most understudied aspects of the carbon budget despite being a substantial proportion of autotrophic respiration, and *c.* 12–25% of total ecosystem respiration (Chambers *et al.*, 2004b; Cavaleri *et al.*, 2006; Malhi *et al.*, 2009). Stem respiration is CO₂ produced by respiration inside the stem that diffuses out radially (Bowman *et al.*, 2008) and is associated with the metabolic activity of plant growth and maintenance

(Malhi *et al.*, 2009). As tree stems consist of several tissues (bark, cortex, phloem, cambium and xylem), which all contain living cells that respire, it can be difficult to measure the respiration rate of individual tissues beneath the stem surface (Teskey *et al.*, 2008; Trumbore *et al.*, 2013). Woody stem CO₂ efflux (EA) to the atmosphere, which is the flux measured at the stem surface, is widely used as a proxy for stem respiration for methodological simplicity, and it is largely a measure of the *in situ* autotrophic respiration of the biologically active outer layer of the stem (Robertson *et al.*, 2010). It is, however, widely acknowledged that there is some uncertainty in the origin of the CO₂ emitted from the stem (Salomón *et al.*, 2024). For example, CO₂ respired inside the stem may be transported away from the origin site upwards in the xylem (Hölttä & Kolari, 2009), and CO₂ originating elsewhere, such as the root system, can also be transported upwards and diffused out within the stem and upper canopy (Teskey *et al.*, 2008; Trumbore *et al.*, 2013).

As stems are the largest contributor to forest biomass, their respiratory consumption has the potential to considerably affect carbon budgets in forest communities (Ogawa, 2006). EA in tropical forests has been shown to be driven by a multitude of factors, with a positive relationship with tree diameter (Meir & Grace, 2002) and growth rate (Katayama *et al.*, 2016; Jardine *et al.*, 2022), and a negative relationship with tree age (Ryan *et al.*, 2004, 2006). As EA is highly reflective of tree metabolism, it can provide vital insights into allocation strategies and response to environmental conditions, particularly if partitioned into its growth and maintenance components. For example, the proportion of maintenance respiration to growth respiration has been found to increase during drought (Rowland *et al.*, 2018). EA has also been shown to decline over elevational gradients (Zach *et al.*, 2008, 2010; Robertson *et al.*, 2010), driven largely by changes in temperature (while also acknowledging the changes in soil nutrients and species composition and structure; Robertson *et al.*, 2010). It is, however, unclear how EA would respond to other environmental gradients such as that of logging disturbance.

In the tropics, most studies on EA have been conducted within old-growth forests (Cavaleri *et al.*, 2006; Katayama *et al.*, 2016; Jardine *et al.*, 2022) with little to no research within logged or degraded tropical forests, despite logged tropical forests being more prominent than old-growth forests across the tropics (Laurance *et al.*, 2014). Gaps left following logging increase light penetration into the canopy, which has been shown to increase competition for this newly available subcanopy light and increase the growth rate of remaining trees (Figueira *et al.*, 2008), and encourage the establishment of pioneer species (DeArmond *et al.*, 2022). Logging removes the larger and more commercially valuable trees, leaving a younger and smaller sized population, changing canopy structure and forest species, age and size composition of the forest. This can cause a shift towards fast-growing light-demanding species from a community dominated previously by slow-growing, conservative and shade-tolerant species (Bischoff *et al.*, 2005). Pioneer species have low-density and low-cost stems (King *et al.*, 2006) with vessel traits displaying resource-acquisition strategies that support fast growth (Jotan *et al.*, 2020). Logging also impacts soils via removal of mineral nutrients through exported logs, soil erosion and leaching (Cleveland *et al.*, 2006) as well as via soil removal, inversion and compaction (Pinard *et al.*, 1996). Such changes have the potential to impact respiratory consumption through a shift in forest structure and growth rate, and subsequently investment strategies. For example, old-growth tropical forest plots have higher values for plant functional traits related to structural stability and persistence, whereas logged plots have greater values for traits that drive carbon capture and growth (Both *et al.*, 2019). Similarly, forest disturbance leads to a higher allocation of carbon towards growth and increased carbon use efficiency (Kunert *et al.*, 2019). Given how expansive logged tropical forests now are, it is imperative to quantify the impact of logging activities on their respiratory fluxes and determine the mechanisms responsible for any observed changes and shifts in respiratory behaviour.

Plot-level studies that use bottom-up field measurements to quantify components of the carbon budget are crucial for

validating and extrapolating respiratory component estimates of forest ecosystems derived from remote sensing or eddy covariance techniques (Robertson *et al.*, 2010). Yet, these field studies are limited due to the technical challenges of sampling continuously, in both space and time (Han *et al.*, 2017). Here, this study reports EA in nine 1-ha forest plots and investigates EA along a gradient from heavily logged to old-growth forest in Sabah, Malaysian Borneo, using EA as a proxy for stem respiration. This study investigates EA at both tree-level and stand-level and focusses on the spatial patterns of EA across these two scales, rather than on temporal variability. By contextualising EA in logged forests, this study adds to the growing pool of research on autotrophic respiration, the least studied component of forest carbon dynamics (Robertson *et al.*, 2010) within this expanding land-use type. Specifically, this study aimed to:

- (1) quantify EA at tree-level and stand-level and determine whether they differ between logged and old-growth plots;
- (2) determine whether allocation of stand-level EA to growth and maintenance respiration, and stem carbon use efficiency differs between logged and old-growth plots;
- (3) investigate the key drivers of tree-level EA in logged and old-growth, including growth rate, tree size and plant functional traits and vessel traits; and
- (4) investigate the key drivers of stand-level EA in logged and old-growth, including carbon allocation, forest structure and composition, and soil nutrients.

Materials and Methods

Study sites

Sampling was conducted within nine 1-ha intensive global ecosystem monitoring (GEM) plots (Marthews *et al.*, 2014; Malhi *et al.*, 2021) in lowland, dipterocarp dominated, humid tropical forest within Sabah, Malaysian Borneo, which captured a gradient of logging intensity from old-growth to heavily logged forest (Table 1). This region is a hotspot for deforestation and forest degradation, with a history of widespread exploitation via selective logging for timber (Pinard *et al.*, 1996; Jomo *et al.*, 2004). The climate is a seasonal, with a mean daily temperature of 26.7°C and *c.* 2600–2700 mm of precipitation annually (Walsh & Newbery, 1999; Kumagai & Porporato, 2012).

Logged plots (five plots) were located within the Stability of Altered Forest Ecosystems (SAFE) Project in the Kalabakan Forest Reserve (Ewers *et al.*, 2011) (Table 1). These plots have been logged two (moderately logged; SAF-03 and SAF-04) or four (heavily logged; SAF-01, SAF-02, SAF-05) times; however, the exact logging history of the plots is not explicitly documented (Struebig *et al.*, 2013; Pfeifer *et al.*, 2015). The first round of logging took place in the mid-1970s, with subsequent rounds during the late 1990s to 2000s (Fisher *et al.*, 2011; Struebig *et al.*, 2013; Pfeifer *et al.*, 2015). Approximately 150–179 m³ ha⁻¹ of timber was removed during this time (Struebig *et al.*, 2013), which is comparable to the mean extraction rate of 152 m³ ha⁻¹ across Sabah (Fisher *et al.*, 2011). As this area was set to be converted to oil palm plantation, the usual logging conventions and 60-year

Table 1 Characteristics of study plots including plot code as it appears in the forestplot.net database, site and coordinates, logging intensity, soil type and topography, basal area ($\text{m}^2 \text{ha}^{-1}$), number of stems, number of big trees, percentage of pioneer species and three most abundant genera.

Plot code	Site and coordinates	Logging intensity	Soil type; topography	Basal area of trees > 10 cm DBH ($\text{m}^2 \text{ha}^{-1}$)	Number of stems > 10 cm DBH	Number of big trees (DBH > 50 cm)	Pioneer species (% of basal area)	Most abundant genera
MLA-01	Maliau Basin Conservation Area, Sabah (4.747°, 1176.970°)	Old-growth	Clay; undulating	41.6 ± 3.59	397	47	0.2 ± 0.3	<i>Dryobalanops</i> , <i>Rubroshorea</i> , <i>Eusideroxylon</i>
MLA-02	Maliau Basin Conservation Area, Sabah (4.754°, 1176.950°)	Old-growth	Clay; moderate slope	34.7 ± 2.74	479	56	1.7 ± 1.2	<i>Parashorea</i> , <i>Mallotus</i> , <i>Rubroshorea</i>
DAN-04	Danum Valley Conservation Area, Sabah (4.951°, 117.796°)	Old-growth	Clay; steep slope	32.0 ± 3.30	444	34	0.7 ± 1.0	<i>Cleistanthus</i> , <i>Diospyros</i> , <i>Parashorea</i>
DAN-05	Danum Valley Conservation Area, Sabah (4.953°, 117.793°)	Old-growth	Clay; flat	30.6 ± 3.37	401	26	0.1 ± 0.0	<i>Diospyros</i> , <i>Aglaia</i> , <i>Syzygium</i>
SAF-03	SAFE Project, Sabah (4.691°, 117.588°)	Moderately logged	Clay; steep slope	19.6 ± 1.88	552	10	21.5 ± 5.0	<i>Rubroshorea</i> , <i>Macaranga</i> , <i>Litsea</i>
SAF-04	SAFE Project, Sabah (4.765°, 117.700°)	Moderately logged	Partly sandy loam, partly clay; flat	19.3 ± 1.70	460	11	6.9 ± 2.2	<i>Syzygium</i> , <i>Vatica</i> , <i>Macaranga</i>
SAF-01	SAFE Project, Sabah (4.732°, 117.619°)	Heavily logged	Clay; mostly flat with a moderate slope on one edge	6.81 ± 1.00	318	1	28.1 ± 4.3	<i>Rubroshorea</i> , <i>Macaranga</i> , <i>Dendrocnide</i>
SAF-02	SAFE Project, Sabah (4.739°, 117.617°)	Heavily logged	Clay; undulating	11.1 ± 1.81	552	0	57.2 ± 5.8	<i>Macaranga</i> , <i>Rubroshorea</i> , <i>Glochidion</i>
SAF-05	SAFE Project, Sabah (4.716°, 117.609°)	Heavily logged	Clay; undulating	19.6 ± 1.88	391	6	34.5 ± 6.6	<i>Dendrocnide</i> , <i>Macaranga</i> , <i>Parashorea</i>

Values are mean ± 1 SE. Species classified as pioneers (based on Köhler *et al.* (2000) and Saner *et al.* (2012)): *Adinandra dumosa* Jack, *Cratoxylum arborescens* Blume, *Dendrocnide elliptica* Chew, *Duabanga moluccana* Bl, *Endospermum peltatum* Merr, *Glochidion borneenses* Boerl, *G. lutescens* Blume, *G. rubrum* Bl, *Ludekia borneensis* Ridsdale, *Macaranga* spp. Thouars, *Mallotus lackeyi* Elmer, *M. mollissimus* Airy Shaw, *M. paniculatus* Müll.Arg, *Melicope lunu-ankenda* T.G. Harvey, *Neolamarckia cadamba* Bosser, *Octomeles sumatrana* Miq, *Pterospermum elongatum* Korth, *P. javanicum* Jungh, *Symplocos fasciculata* Zoll.

rotation period were not followed. As a result, large parts of this area were left highly degraded (Reynolds *et al.*, 2011), and the current aboveground carbon stocks are now estimated at *c.* 70% and *c.* 25% of the prelogging 1970 's aboveground carbon stocks in moderately and heavily logged plots, respectively (Riutta *et al.*, 2018). As the data from this study are derived from continuous measurements between 2011 and 2019, the heavily logged plot estimates represent *c.* 10-yr recovery and moderately logged at *c.* 20-yr recovery. Within these logged plots, pioneer species (determined based on Köhler *et al.* (2000) and Saner *et al.* (2012); see footnote of Table 1) contributed 30% of basal area on average (Table 1). Old-growth plots were located within Maliau Basin Conservation Area (two plots) and Danum Valley Conservation Area (two plots) (Table 1). Within these plots, there is no evidence of direct human disturbance or logging. Pioneer species contributed *c.* 0.7% of basal area. For more detailed site and plot descriptions, including species composition, stem

diameter distribution, soil properties and a map, see Riutta *et al.* (2018).

Stem CO₂ efflux measurements

Stem CO₂ EA was measured with a static chamber technique using standardised techniques from the GEM protocol (Marthews *et al.*, 2014; Malhi *et al.*, 2021). Campaigns were conducted approximately monthly between 2011 and 2019 for SAFE Project and Maliau Basin Conservation Area plots, and between 2015 and 2019 for plots in Danum Valley. These campaigns were, however, intermittent due to various issues with access, staffing and equipment. Approximately 50 trees were sampled per 1-ha plot, and these were of various sizes and species, and distributed evenly around the plot (Supporting Information Figs S1, S2). Not all trees were measured in each campaign due to fallen respiration collars and mortality. Once a year, new trees

were selected for sampling to replace trees in the sample that had died. As the data collection was part of a long-term carbon monitoring campaign (Mills *et al.*, 2023), and due to the accessibility of the plots and battery life of the equipment, it was not possible to quantify diurnal or vertical variation in EA within this study. To control for temporal systematic error, sampling was conducted within the same time frame across all plots (09:00 h–14:00 h), and the trees were measured in different orders across the visits.

On each sampled stem, a PVC collar with a 10.6 cm internal diameter and 5 cm height was installed at 1.1 m height with silicone sealant (Fig. S3). CO₂ EA from the stem was then measured with an IRGA (EGM-4; PP Systems) and soil respiration chamber (SCR-1; PP Systems). A custom ring adapter of 11 cm diameter and 3.5 cm height was fitted to the chamber to match the diameter of the collars and enable an air-tight seal to avoid leakage (Marthews *et al.*, 2014). Before commencing each measurement, the chamber was flushed, and collar fanned to remove stagnant air. Any mosses, epiphytes or insect nests were also removed from the collar before each measurement. The chamber was then placed onto the collar, CO₂ EA was measured for 120 s, and air temperature was measured at the stem surface. Over the 120 s, CO₂ accumulates in the chamber and the uncorrected CO₂ flux (R_u ; ppm s⁻¹) is calculated by the IRGA by fitting a linear regression between CO₂ concentration and time (mean $R^2 = 0.87$). The CO₂ flux is then calculated using the ideal gas law (Marthews *et al.*, 2014):

$$EA = \frac{R_u \times M \times P \times V}{R \times (T + 273.15)} \times \frac{TC}{A}$$

where R_u is the uncorrected flux (as volume fraction), M is the molar mass of carbon (12.01), P is ambient pressure (Pa), V is the volume m³ (total volume of the chamber, adapter piece and respiration collar), R is gas constant (8.134), T is air temperature near stem surface (°C), A is the area of the collar (m²) and TC is time conversion, in this case from second to month to give EA of each tree in g C m⁻² Stem Area month⁻¹. One measurement per tree was taken, unless leakage was detected and then the measurement was repeated, and campaigns were repeated monthly throughout the measuring period. Data from 2016 were removed from the dataset as the region experienced a strong El Niño event during this year – the focus of this paper was spatial variability across trees and plots, rather than temporal patterns. Ollech–Webel seasonality test, performed using R package SEASTEST (Ollech, 2021), found no significant interannual patterns in the data from before or after 2016 ($P = 0.6$; $P = 0.5$, respectively). Data were corrected to 25°C assuming a Q₁₀ of 2.0 (Cavaleri *et al.*, 2006).

Tree-level EA and explanatory variables

Observed EA data were subject to quality control and outlier detection, removing spurious data that were considered to be due to mechanical issues, human error or to be outside logical bounds. This included large negative values that indicated leakage

that was not detected during the measurements. Observations outside the 2.5 and 97.5 percentiles within each plot were examined and removed if they were also outliers among the observations of that day, and for that particular stem across all campaigns. EA observations of each tree were then averaged to provide an estimate of tree-level EA over the course of the study. Only trees with at least two repeated flux measurements and two repeated forest censuses were included in the final dataset. The final dataset following quality control consisted of 4381 individual observations of EA from 347 trees, 189 of which were trees from logged plots and 158 from old-growth plots. Each tree was measured 13 times on average (range 2–33).

Growth rate (cm yr⁻¹) for individual trees was calculated from diameter increase using diameter at breast height (DBH; at 1.3 m) from a biannual forest census (Riutta *et al.*, 2018). Plant functional traits (Both *et al.*, 2019) and wood anatomy traits (Jotan *et al.*, 2020) were collected in a campaign in 2015 (Table S1) across eight plots; SAF-05 plot was not sampled. Leaf and wood trait analyses followed standardised protocol (Pérez-Harguindeguy *et al.*, 2013). Briefly, mature undamaged leaves were collected from fresh-cut branches and cleaned, and leaf weight, area, thickness and dry matter content force to punch and branch wood density were determined in a field laboratory. Dried bulked and milled leaf material samples were used for nutrient and isotope concentrations (Ca, K, Mg, P, C, N, δ¹⁵N, δ¹³C, cellulose, hemicellulose and lignin), and analysis of phenols, tannins and pigments was conducted on 0.7-cm-diameter leaf discs from fresh leaves (for more information, see Both *et al.*, 2019). Wood anatomy and vessel trait measurements involved analysis of branch sections using imagery of cross sections to determine anatomical traits such as vessel area, vessel lumen fraction, vessel number per area, hydraulically weighted diameter and potential hydraulic conductivity (for more information, see Jotan *et al.*, 2020). The dataset where both EA and functional traits were available consisted of 86 trees, 45 were from logged plots and 41 from old-growth plots.

Stand-level EA and explanatory variables

To quantify stand-level EA (Mg C ha⁻¹ yr⁻¹) for each 1-ha plot, the mean EA of the sampled trees per month per plot was scaled to the total stem surface area (m²) of each 1-ha plot, which is the sum of surface area (SA) of trunks and larger branches of trees > 10 cm in diameter, calculated using an allometric equation based on stem diameter (Chambers *et al.*, 2004b):

$$SA = 10^{-0.105 - 0.686X + 2.208X^2 - 0.627X^3}$$

where $X = \log_{10}(\text{DBH in cm})$, which is derived from tree census data (Riutta *et al.*, 2018). Total stem surface area index (SAI) expresses stem area as unitless (m² of stem area per m² of ground area).

Stand-level EA was partitioned into growth and maintenance respiration (Mg C ha⁻¹ yr⁻¹) using a linear equation (Ryan *et al.*, 2009; Robertson *et al.*, 2010). This method assumes that woody stem CO₂ EA represents woody respiration, and so

tree-level EA (scaled to $\text{g C m}^{-2} \text{yr}^{-1}$) is regressed against biomass growth ($\text{g C m}^{-2} \text{yr}^{-1}$) per individual tree within each plot. Biomass growth was estimated by calculating aboveground woody biomass of each stem from allometric equations for moist tropical forest with diameter, height and wood density (Chave *et al.*, 2005), and calculating biomass gain between biannual forest censuses. Stand-level maintenance respiration was estimated as the y -intercept of the linear equation, as this represents woody respiration when the trees are not growing, and stand-level growth respiration was estimated as the difference between stand-level EA and maintenance respiration (Amthor, 1989). The SE of maintenance respiration was estimated as the SE of the y -intercept. Root sum of squares was used to calculate the error of growth respiration using the error of the y -intercept and stand-level EA SE (Robertson *et al.*, 2010).

Stem carbon use efficiency (CUE) for each 1-ha plot was calculated as $\text{NPP}_{\text{stem}}/(\text{NPP}_{\text{stem}} + \text{stand-level EA})$, whereby NPP_{stem} is stand-level woody stem productivity ($\text{Mg C ha}^{-1} \text{yr}^{-1}$), which was estimated from the increase in aboveground woody biomass between two subsequent censuses (Riutta *et al.*, 2018; Mills *et al.*, 2023). Soil characteristics (total Mg, P, Ca, Na^+ , K^+ , Al^+ and pH) for each plot were measured in the 0-to 10-cm soil layer using three replicas per plot and following standardised RAINFOR protocols (Table S1) (Quesada *et al.*, 2010; Riutta *et al.*, 2021).

Statistical analyses

All statistical analyses were conducted in R (v.4.0.2; R Core Team, 2024). To determine the difference in tree-level EA and tree-level growth rate (cm yr^{-1}) between forest types (old-growth and logged), Wilcoxon signed-rank tests were applied. To investigate the role of growth and tree size (DBH) on tree-level EA, a generalised linear model (GLM) was applied with a gamma family distribution (respiration value are positive, variance increases with increasing mean), with logarithmic link function; plot code as a random effect did not improve the model. To examine whether EA differed between pioneer and nonpioneer species (Table 1), when controlling for tree size, a linear mixed-effect model between tree-level EA and pioneer status and DBH with plot code as a random effect was applied, using the package NLME (Pinheiro *et al.*, 2023). This model was for logged plots only, as the proportion of pioneers was negligible in the old-growth plots (range: 0.1–1.7% of plot BA). The same model structure was used with tree-level growth rate as the response variable to determine the influence of the pioneer species on tree-level EA and tree-level growth rate.

A multivariate partial least squares regression (PLS-R) was employed to investigate the drivers of tree-level EA and their combined effects, conducted in R package MDATools (Kucheryavskiy, 2020). PLS-R is a multivariate method recommended for analyses where there are multiple explanatory variables and multicollinearity is likely; it reduces the input variables into components, while reducing the dimensionality of correlated variables, which are then used for the regression (Zema *et al.*, 2023). For this analysis, separate models were constructed for trees in

logged and old-growth plots, and growth rate (cm yr^{-1}), DBH (cm), subplot basal area (m^2 per 20 m \times 20 m subplot minus the basal area of the target tree, as a proxy for competition), plant functional traits that are associated with leaf nutrients ($\delta^{15}\text{N}$, Ca, Mg, K, N, P), photosynthesis ($\delta^{13}\text{C}$, carotenoids, specific leaf area) and structure (lignin, cellulose, hemicellulose and leaf thickness) (Both *et al.*, 2019), and wood anatomy and vessel traits (wood density, vessel area, vessel lumen fraction, vessel number per area, hydraulically weighted diameter and potential hydraulic conductivity; Jotan *et al.* (2020)) were used as input variables (Table S1). Leave-one-out cross-validation was used to select the optimum number of components and root-mean-squared error (RMSE) and the coefficient of determination (R^2) was used to evaluate model performance. Outlier detection and removal was conducted (Rodionova & Pomerantsev, 2020), and variable importance projection (VIP) scores were used for variable selection, with a criterion of > 1 (Trap *et al.*, 2013; Xu *et al.*, 2021). All the variables were scaled to have a mean of 0 and a SD of 1, thus allowing the comparison of variables of different units. Only trees that were sampled in both the plant functional trait (Both *et al.*, 2019) and wood anatomy campaign (Jotan *et al.*, 2020) were included in the PLS-R model, resulting in 86 trees, 45 from logged plots and 41 from old-growth plots.

Difference in stand-level EA, allocation to maintenance and growth respiration, CUE and SAI between forest types (old-growth vs logged) was determined using Wilcoxon signed-rank tests and t -tests. Relationships between stand-level EA, forest type and plot basal area (BA; $\text{m}^2 \text{ha}^{-1}$), and stand-level EA, forest type and SAI, were investigated using multiple linear models. The relationship between stand-level EA and CUE, and CUE with BA and growth and maintenance respiration was investigated using multiple linear models. The relationships between stand-level EA and soil characteristics (total Mg, P, Ca, Na^+ , K^+ , Al^+ and pH) were investigated using multiple linear models, as well as these soil traits with BA, SAI and woody stem NPP.

Results

Tree-level EA

This study quantified tree-level EA of 347 trees across both logged and old-growth forests. Tree-level EA was higher in logged ($37.0 \pm 1.1 \text{ g C m}^{-2} \text{month}^{-1}$) than in old-growth ($26.92 \pm 1.14 \text{ g C m}^{-2} \text{month}^{-1}$) plots ($W = 21\,209$, $P < 0.001$; Fig. 1b), but there was no difference in tree-level EA between moderately and heavily logged plots ($P = 0.75$). Logged plots had higher growth rate than old-growth plots ($W = 19\,374$, $p = < 0.001$) with an average of 0.78 ± 0.05 vs $0.47 \pm 0.05 \text{ cm yr}^{-1}$, respectively. A GLM with DBH, growth rate and forest type (logged vs old-growth) explained 24% of the variation in tree-level EA. Tree-level EA had a positive relationship with DBH ($P < 0.001$) and growth rate ($P < 0.001$), with no interaction between the variables ($P = 0.58$) (Fig. 2a,b). While EA was higher in logged than in old-growth plots ($P < 0.001$), there was no interaction between forest type and DBH ($P = 0.37$) or forest type and growth rate ($P = 0.15$). Within logged plots,

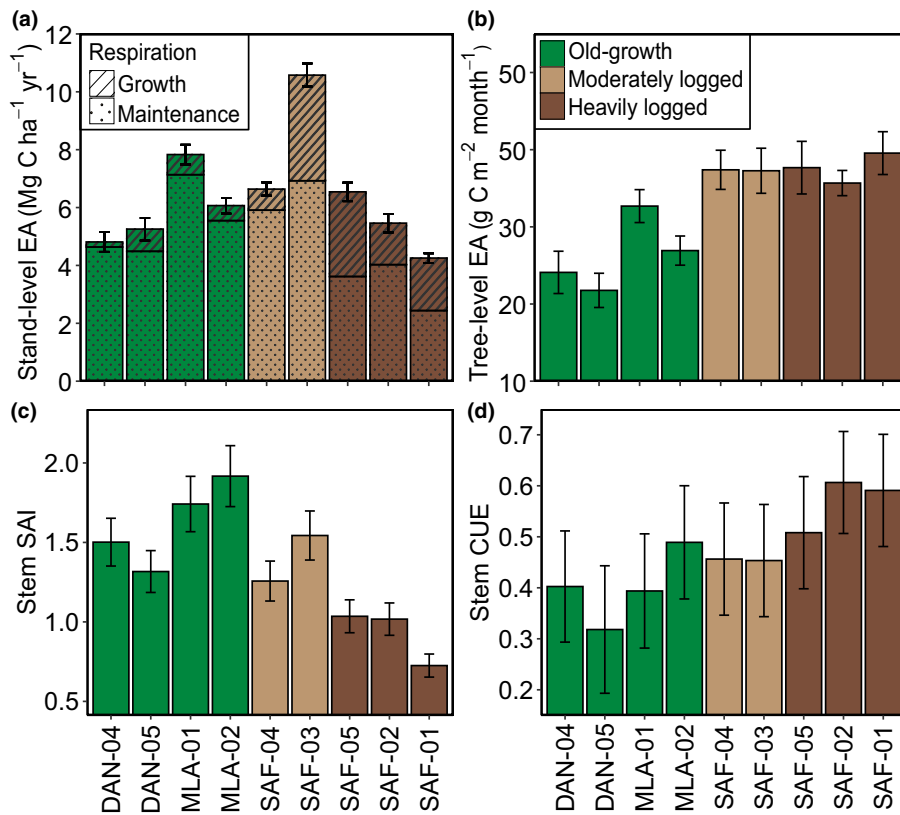


Fig. 1 Stand-level stem CO₂ efflux (EA) along the logging gradient from old-growth (green) to moderately (twice logged; light brown) and heavily logged (four times logged; dark brown), with EA partitioned into maintenance (dotted) and growth (lines) respiration. There was no difference in stand-level EA between logged and old-growth plots (*T*-test; $P = 0.59$). Error bars represent propagated SE of stand-level EA (a). Mean tree-level EA, with SE, along the logging gradient, whereby tree-level EA was significantly higher in logged than old-growth plots (Wilcoxon signed-rank test; $P < 0.001$, b). Stem surface area index (SAI) along the logging gradient with error bars that represent surface area index error, which was assigned as 10% based on the uncertainty in allometry based on Robertson *et al.* (2010). SAI was significantly higher in old-growth than logged plots (*T*-test; $P = 0.03$, c). Stand-level stem carbon use efficiency (CUE), which was calculated as woody stem net primary productivity/(woody stem net primary productivity + stand-level EA), along the logging gradient. Stem CUE was significantly higher in logged than old-growth plots (*T*-test; $P = 0.039$). Error bars represent propagated SE of stand-level CUE (d). For plot codes, see Table 1.

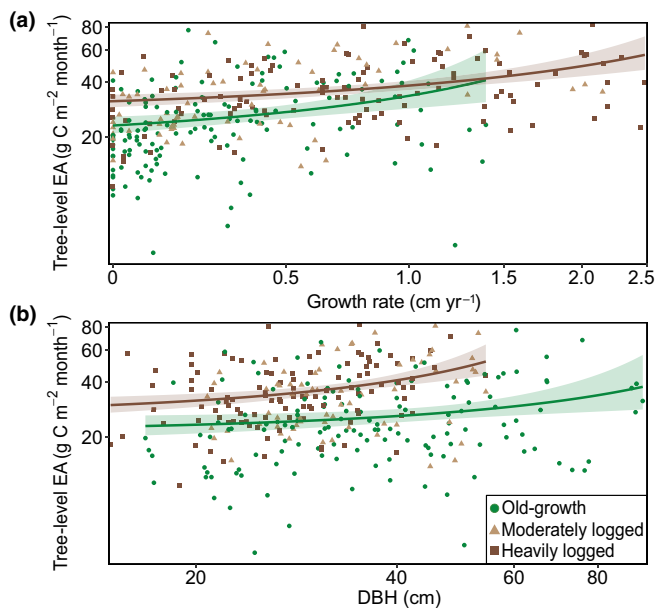


Fig. 2 Tree-level stem CO₂ efflux is higher in logged than old-growth plots ($P < 0.001$). Tree-level EA increases with increasing growth rate ($P < 0.001$); (a) and with tree diameter at 1.3 m height (DBH; $P < 0.001$); (b), as determined by a generalised linear model. Axes are shown with logarithmic scaling. Brown line represents logged plots (moderately logged—light brown triangles; heavily logged—dark brown squares) and green line represents old-growth plots (green circles), with $\pm 95\%$ confidence intervals.

there was no difference in tree-level EA of pioneer species vs non-pioneer species ($P = 0.32$) despite the higher growth rate of pioneer species (when controlling for tree size; $t(187) = 2.14$, $P = 0.03$) of 0.96 ± 0.1 vs 0.70 ± 0.06 cm yr⁻¹ of pioneers vs nonpioneers in logged plots, respectively. In old-growth plots, none of the sampled trees were pioneers as their average contribution to total basal area is only 0.7%.

The potential direct and indirect spatial drivers of tree-level EA were examined using a PLS-R model. The PLS-R model for logged forests had an $R^2 = 0.51$ with an optimum number of components of 2, which explained 76.4% cumulative variance in X and 51.0% cumulative variance in Y (Fig. 3a,b; Table 2). Growth rate (cm yr⁻¹) was significant in both components ($P = 0.02$; $P = 0.04$) and had the highest coefficients and VIP score. In Component 1, $\delta^{15}\text{N}$ was significant ($P = 0.02$) and total P was significant in Component 2 ($P = 0.04$). This model had high contribution from variables that relate to vessel structure and wood anatomy (vessel lumen fraction, wood density and number of vessels) as well as leaf strength and structure (tannins, leaf thickness and cellulose) although these variables were not significant (Table S2). Most variables displayed positive coefficients, apart from $\delta^{15}\text{N}$, P , tannins and cellulose (Fig. 3a,b). The old-growth PLS-R model had a lower R^2 of 0.33 with an optimum number of components of 1, which explained 73.8% cumulative variance in X and 32.6% cumulative variance in Y (Fig. 3c,d; Table 2). In this model, DBH (cm) and hemicellulose had the highest VIP score and coefficients and were significant within

Fig. 3 Partial least squares regression (PLS-R) variable importance projection scores (a, c) and coefficients (b, d) for the variables that influence tree-level stem CO₂ efflux (EA) in logged (brown) and old-growth (green) forest plots. Asterisk (*) indicates variables that were significant within the model as determined by Jack-knifing ($P < 0.05$), solid outline represents coefficients from Component 1 (b, d) and dashed outline represents coefficients from Component 2 (b). Trait acronyms and abbreviations are as follows, whereby $\delta^{15}\text{N}$ is foliar 15N isotope, P_m is foliar phosphorus content, lumen fraction is vessel lumen fraction, N. Vessels is number of vessels within wedge, DBH is stem diameter at 1.3 m height, $\delta^{13}\text{C}$ is foliar 13C isotope, subplot BA is the basal area of trees in a 20 × 20 m subplot minus the basal area of the target tree (as a proxy for competition) and N_{pa} is foliar nitrogen. Subscripts 'pa' and 'm' indicate units per leaf area (mg mm^{-2}) and per leaf dry mass (mg g^{-1}), respectively. Further variable descriptions can be found in Supporting Information Table S1 and output in Table S2.

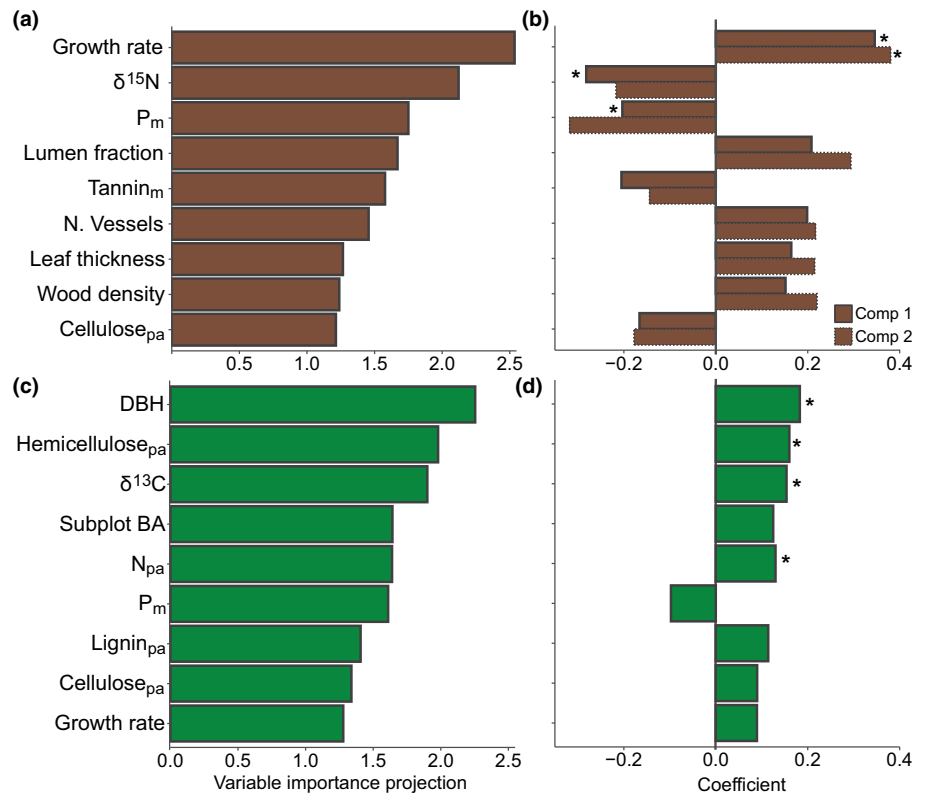


Table 2 Summary of the best supported partial least squares regression models for tree-level stem CO₂ efflux (EA; $\text{g C m}^{-2} \text{ month}^{-1}$) within logged and old-growth, whereby RMSE is root-mean-squared error of prediction and CV is cumulative variance explained (%) (Supporting Information Table S2).

Model	Optimum components	R^2	CV in X	CV in Y	RMSE
Logged plots	2	0.51	76.4	50.9	9.02
Old-growth plots	1	0.33	73.8	32.6	11.1

the model ($P = 0.002$; $P = 0.01$). $\delta^{13}\text{C}$ and N were also significant variables within the model ($P = 0.02$; $P = 0.03$). This model has a high contribution from variables related to leaf structure and strength (hemicellulose, cellulose and lignin) and photosynthesis (N, $\delta^{13}\text{C}$) (Fig. 3c,d; Table 2), growth rate and subplot basal area were also included in the model but were not significant (Table S2). In common with the logged model, P had a negative coefficient and, therefore, a negative influence on tree-level EA.

Stand-level EA

There was no difference in stand-level EA between logged and old-growth plots ($P = 0.59$), with an average of $6.0 \pm 0.7 \text{ Mg C ha}^{-1} \text{ yr}^{-1}$ in old-growth plots and $6.7 \pm 1.1 \text{ Mg C ha}^{-1} \text{ yr}^{-1}$ in logged plots (Fig. 1a). Due to the higher tree-level EA (Fig. 1b),

logged plots exhibited similar stand-level EA to old-growth plots, despite having reduced SAI ($t(7) = -2.6$, $P = 0.03$) (Fig. 1c) and BA ($\text{m}^2 \text{ ha}^{-1}$; $t(6.5) = -4.8$, $P = 0.002$; Table 1; Fig. S2). There was no significant difference in the total number of stems ($> 10 \text{ cm DBH}$) between the two forest types ($P = 0.94$), but the diameter distribution differed: Logged forest plots had significantly more smaller 20–30-cm trees ($t(6.7) = 2$, $P = 0.042$) than old-growth plot, and old-growth plots had significantly more larger trees of 60–70 cm ($t(3.6) = -2.4$, $P = 0.041$) and $> 70 \text{ cm}$ ($t(4.7) = -6$, $P = 0.001$; Fig. S2).

There was a significant difference in how EA was allocated to growth and maintenance respiration. Logged forest plots had higher allocation to growth respiration ($t(4.5) = 2.9$, $P = 0.04$), which was $21.7 \pm 6.2\%$ of stand-level EA relative to $8.9 \pm 2.2\%$ within old-growth plots (Fig. 1a). Allocation of stand-level EA to maintenance respiration ranged from 55.3 to 96.0% across all study plots, with an average $91.0 \pm 2.2\%$ and $68.0 \pm 6.2\%$ in old-growth and logged plots, respectively (Fig. 1a). Stem CUE was higher ($t(7) = -2.6$, $P = 0.039$) in logged plots (0.52 ± 0.11) than in old-growth plots (0.40 ± 0.11) (Fig. 1d), with no significant linear relationship between stem CUE and stand-level EA ($P = 0.60$).

Stand-level EA was positively correlated with forest type and plot BA ($R^2 = 0.51$, $P = 0.05$; Fig. 4a) and SAI ($R^2 = 0.61$, $P = 0.026$; Fig. 4b). For a given BA and SAI, EA was higher in logged plots than in old-growth plots (Figs 4a,b, S4). Stem CUE and maintenance respiration, on the other hand, showed a universal pattern across both forest types, as CUE negatively

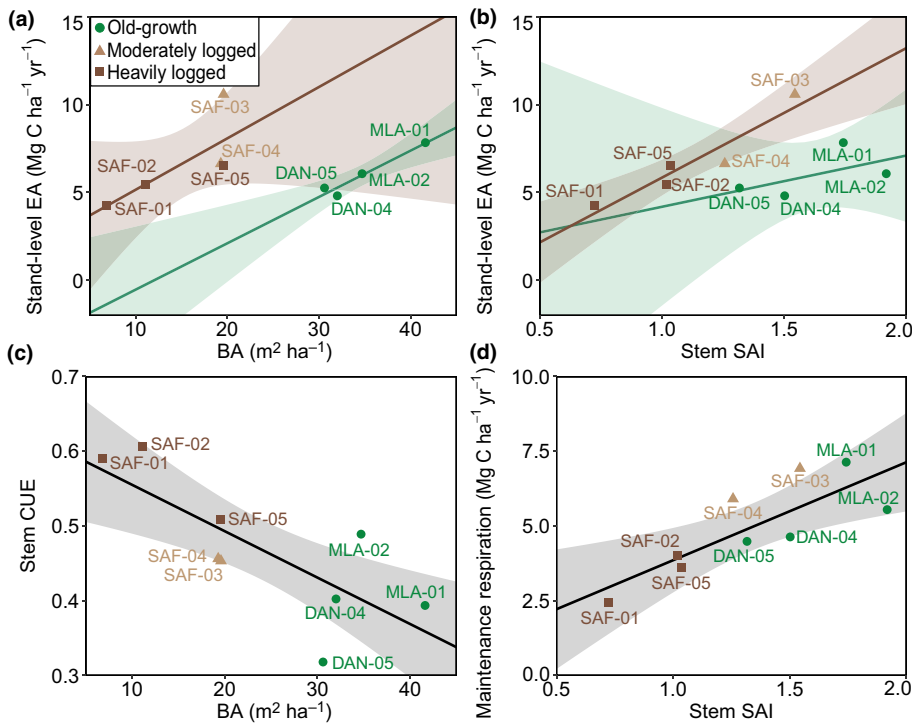


Fig. 4 Linear model between stand-level stem CO₂ efflux (EA) and basal area (BA) by forest type (old-growth, green; logged, brown) ($R^2 = 0.51$, $P = 0.05$) (a). Linear model between stand-level EA and stem surface area index (SAI) by forest type ($R^2 = 0.61$, $P = 0.026$) (b). Stand-level stem carbon use efficiency declines with increasing BA (c; $R^2 = 0.53$, $P = 0.02$). Stand-level maintenance respiration increases with increasing stem SAI (d; $R^2 = 0.59$, $P = 0.009$). Error band represent 95% CI and old-growth plots are represented by green circles, moderately logged plots by light brown triangles, and heavily logged plots by dark brown squares. For plot codes, see Table 1.

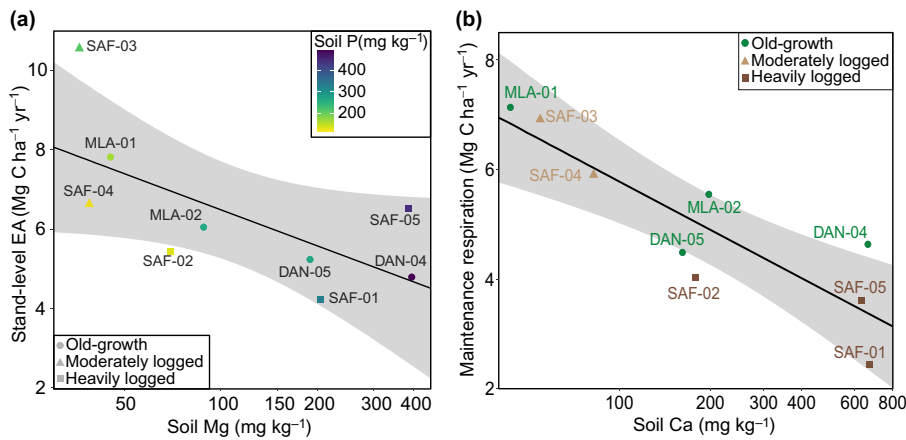


Fig. 5 Stand-level stem CO₂ efflux declines with increasing soil magnesium and soil phosphorus (a; $R^2 = 0.63$, $P = 0.02$), and maintenance respiration declines with increasing soil calcium (b; $R^2 = 0.73$, $P = 0.002$). Explanatory variables are log-transformed, x-axes are shown with logarithmic scaling and error bands represent $\pm 95\%$ confidence interval. Old-growth plots are represented by circles, moderately logged plots by triangles and heavily logged plots by squares. For plot codes, see Table 1.

correlated with BA ($R^2 = 0.53$, $P = 0.02$; Fig. 4c) and maintenance respiration positively correlated with stem SAI ($R^2 = 0.59$, $P = 0.009$; Fig. 4d).

Soil Mg (log-transformed) and soil P displayed a negative relationship with stand-level EA ($R^2 = 0.63$, $P = 0.02$; Fig. 5a). Soil Ca (log-transformed) also had a negative relationship with both stand-level EA ($R^2 = 0.46$, $P = 0.03$) and with maintenance respiration ($R^2 = 0.73$, $P = 0.002$; Fig. 5b). These relationships with soil nutrients were not mediated via stand structure or growth: Soil Mg, soil P and soil Ca were not correlated with BA ($P = 0.89$; $P = 0.86$; $P = 0.17$), woody stem NPP ($P = 0.21$; $P = 0.35$; $P = 0.59$) or SAI ($P = 0.34$; $P = 0.73$; $P = 0.16$). A principal component analysis was conducted to assess whether soil characteristics in combination (including N, P, Mg, Ca, pH, Na⁺, K⁺, Al⁺) rather than individually would constitute a

stronger predictor for stand-level EA, but there was no significant relationship with the strongest axis and stand-level EA (Fig. S5).

Discussion

This study quantified EA at tree-level and stand-level and reported different patterns of EA along the logging gradient in Bornean tropical forests. While tree-level EA was higher per unit of stem area in logged plots, old-growth plots had higher total stem surface area; thus, there was no observed difference in stand-level EA between forest types. Average stand-level EA across the study plots was similar to previous studies across the tropics, including Puerto Rico (2.14–7.37 Mg C ha⁻¹ yr⁻¹; Harris *et al.*, 2008), the Peruvian Amazon (6.45 ± 1.12 Mg C ha⁻¹ yr⁻¹; Robertson *et al.*, 2010), the Brazilian Amazon

($7.07 \pm 0.72 \text{ Mg C ha}^{-1} \text{ yr}^{-1}$; Rowland *et al.*, 2018) and elsewhere in Malaysian Borneo ($7.06 \pm 2.09 \text{ Mg C ha}^{-1} \text{ yr}^{-1}$; Katayama *et al.*, 2016). Stand-level EA contributed 23–42% of autotrophic respiration and 12–23% of total ecosystem respiration (Mills *et al.*, 2023), consistent with previous estimates in tropical forests (Chambers *et al.*, 2004b; Cavaleri *et al.*, 2006; Malhi *et al.*, 2009).

Although there was no difference in stand-level EA between the forest types, there was a difference in how EA was allocated and, therefore, a difference in investment priorities. While maintenance respiration dominated in both forest types, old-growth plots allocated more towards maintenance respiration than logged plots. This was due to their higher SAI; the relationship between maintenance respiration and SAI was consistent across the forest types, indicating a similar fixed cost per unit stem area. In logged plots, by contrast, there was increased allocation to growth respiration and priority for growth, likely attributed to the increased light availability following logging and trees favouring wood production and prioritising vertical stem growth to avoid becoming overtopped by their neighbours (Chen *et al.*, 2013; Riutta *et al.*, 2018). Furthermore, higher stem CUE was observed in logged vs old-growth plots; that is, production of new woody tissue had a lower metabolic cost in logged plots. This could be due to trees investing less into defence within younger disturbed forests (Kunert *et al.*, 2019) and due to the higher abundance of fast-growing early successional species with low wood density. The higher CUE in logged plots is also consistent with the observed NPP allocation shift towards wood production at the expense of leaf production (Riutta *et al.*, 2018). Figueira *et al.* (2008) also reported a marked increase in wood carbon use efficiency in an Amazonian forest following logging, particularly for small trees, although the values are not directly comparable with this study, as they expressed wood CUE as the ratio of wood production to GPP. The observed stem CUE for old-growth plots in this study, 0.40 ± 0.11 , is similar to that in Central Amazonia of *c.* 0.43 (Chambers *et al.*, 2004b).

This study also investigated the key drivers of EA at both tree-level and stand-level. At both levels, EA was driven by differences in investment strategies, which were induced by disturbance. At stand-level, SAI and BA were strong predictors of EA for both forest types, reflective of differences in forest structure. In logged plots, there is an absence of larger trees and higher gap frequency (Riutta *et al.*, 2018), and most of their total BA is made up by smaller and medium-sized trees (Fig. S2). These smaller and medium-sized trees benefit from increased light availability and decreased competition for resources following logging, and so growth rate increases (Chambers *et al.*, 2004a; Figueira *et al.*, 2008). Here, the effect of changes in forest structure and investment strategies are interlinked, as increased allocation to growth respiration in logged plots is likely associated with differences in forest structure and light availability that translate into changes in species composition and growth rate that drive the measured differences in EA. This indicates the presence of two alternative metabolic states. In the 'logged forest state', growth is prioritised by almost all trees, and in the 'old-growth state',

maintenance is prioritised, which is reflective of the growth and maintenance respiration allocation observed (Fig. S4).

At stand-level, EA was influenced by soil characteristics across both forest types. The results show that stand-level EA decreased with higher concentrations of Mg and P, with Mg playing a vital role in the availability of P (Mam Rasul *et al.*, 2011), and maintenance respiration negatively correlated with soil Ca. Although research into the direct relationship between EA and soil nutrients is limited, these results would suggest higher stand-level EA on nutrient-poor soils. Mg and K deficiency have been shown to increase leaf dark respiration, likely due to upregulated maintenance respiration and increased metabolism to counter the nutrient deficiencies (Li *et al.*, 2017; Rogiers *et al.*, 2020). The scarcity of soil P may result in higher metabolic cost of wood production, and/or shift in NPP allocation towards wood at the expense of leaf and fine root tissues, which have a higher P concentration than woody tissue. Tree species that persist on low fertility soils have denser wood and lower wood P concentration, which is potentially a coordinated evolution of traits to facilitate survival on low-resource habitats (Heineman *et al.*, 2016). Ca depletion inflicts significant stress on trees, which causes an upregulation in water-use efficiency (Oulehle *et al.*, 2023) as Ca contributes to regulating stomatal aperture (Lanning *et al.*, 2019). This may suggest a higher metabolic cost of the upward transport of solutes under Ca depletion, which could potentially contribute to the increased stand-level maintenance respiration. Furthermore, Ca is a key element in wood formation, affecting xylem structure, cambial width and lignification (Fromm, 2010). As the exact mechanisms for the link between EA and soil nutrients are not well-understood or -studied, these are just a few proposed explanations for the observed trends.

At tree-level, growth and tree size were moderate drivers of tree-level EA in both forest types. Previous studies have reported a decline in both EA and with increasing tree age and size, at the scale of individual trees (Ryan *et al.*, 2006) and tree stands (Ryan *et al.*, 2004). The reported decline in EA with tree size exceeded the decline in growth and may be induced by a decrease in radial diffusion through the bark and/or higher sapflow transporting CO_2 away from the origin site (Ryan *et al.*, 2004) as stem allometry plays an important role in CO_2 efflux due to differences in relative fractions of metabolically active tissues between trees of different diameter sizes (Pruyn *et al.*, 2002, 2003; Rodríguez-Calcerrada *et al.*, 2015). However, within these study plots, a decline in tree-level EA with size was not observed; rather, there was a steady increase in both growth and tree-level EA with tree size in both forest types. This supports the idea that some of the very largest trees in a stand can still maintain a high growth rate (Piovesan & Biondi, 2021). The model had fairly low predictive power ($R^2 = 0.24$), which is consistent with previous studies in Central ($R^2 = 0.3$, Jardine *et al.*, 2022; $R^2 = 0.35$, Chambers *et al.*, 2004b) and Eastern Amazon ($R^2 = 0.38$, Rowland *et al.*, 2021), indicating that other variables influence both tree-level EA and growth. For example, while pioneer species had higher growth rate, there was no difference in tree-level EA compared with nonpioneer species, likely attributed to the

low-density, low-cost stems of the pioneers (King *et al.*, 2006). Post logging, pioneer species have been found to grow two to five times faster than commercial species (DeArmond *et al.*, 2022) – this, however, does not translate into an equally large difference in woody biomass production, due to their low wood density (*c.* 0.39 vs 0.53 g cm⁻³ for pioneer and nonpioneer species, respectively, in the logged plots; species-specific wood density estimates from Zanne *et al.*, 2009). It is not, however, only pioneer species that display increased growth rates, as species found in both forest types grow significantly faster in logged than in old-growth plots (Riutta *et al.*, 2018). Previous research has also found no taxonomic signal in stem respiration (Rowland *et al.*, 2018) or growth rate (Rowland *et al.*, 2021), indicating that forest structure, increased light and reduced competition are more important than species identity for EA.

Differences in investment strategies are also present at tree-level. In both PLS-R models, foliar P had a negative influence, indicating a higher metabolic cost of wood production with depleted P. The logged model had a high contribution from growth rate and from traits related to wood anatomy and vessel structure. In Amazonia, wood anatomy has been shown to be influenced by the environmental conditions in disturbed vs undisturbed stands when comparing between the same tree species (Campbell *et al.*, 2016). Furthermore, pioneer species possess vessel traits that reflect the need to capture and transport resources to support their faster growth rates (Jotan *et al.*, 2020). This may indicate that the link between tree-level EA and wood anatomy could be a function of investment strategies, that is to support faster growth. Additionally, within the logged plots, foliar $\delta^{15}\text{N}$, tannins and cellulose have negative coefficients. Since some of these traits relate to more maintenance purposes (as tannins contribute to defence, cellulose to leaf structure), this could indicate that trees in logged plots that invested in such maintenance did so at a trade-off with growth, and so had a lower EA, respectively.

Within the old-growth model, the most important variables were tree size and traits that relate to leaf structure and strength (foliar hemicellulose, cellulose and lignin), indicating that tree-level EA in old-growth plots was a function of investment in maintenance and cell structure, and increased with tree size. Furthermore, photosynthetic traits of foliar $\delta^{13}\text{C}$ and N were important within the old-growth model but not present within the logged model. As previous research has found lower $\delta^{13}\text{C}$ in leaves from shaded sites compared with lighter sites (Vitoria *et al.*, 2016), and given the importance of tree size in this model, this could indicate increased EA from the largest trees with greatest access to light. Subplot basal area, as a proxy for competition, was also important within the old-growth model and had a positive coefficient, similar to stand-level with increased EA with increasing basal area, but this was not significant within the model. As the two models had different variables of importance, the results show how logging activities impact investment priorities. Given that independent trait patterns exist within both logged and old-growth forest (Both *et al.*, 2019), it is challenging to disentangle whether the observed patterns are related to tree-level EA or are reflective of underlying trait patterns within each forest type. However, this may also be indicative of how the

difference in trait patterns is reflected in respiratory consumption and suggests that leaf and wood anatomy traits can be used in predictive models for EA.

This study quantified EA at both tree-level and stand-level along a logging gradient in Malaysian Borneo and demonstrated how the different investment strategies are reflected in both tree-level and stand-level EA. This study provides one of the most extensive records of EA in the tropics, to the best of our knowledge. Thus, by contextualising EA in logged forests, these results add to the growing pool of research on autotrophic respiration, the least studied component of forest carbon dynamics within an understudied, yet expanding, land-use.

Acknowledgements

This study was part of the SAFE Project, the Global Ecosystems Monitoring network (gem.tropicalforests.ox.ac.uk) and Imperial College's Grand Challenges in Ecosystems and the Environment Initiative. We acknowledge funding from the Sime Darby Foundation and the Biodiversity and Land-use Impacts on tropical ecosystem function (BALI) Project (NE/K016377/1) within the Natural Environment Research Council Human-Modified Tropical Forests Programme. MBM was supported by NERC studentship awarded through the Central England NERC Training Alliance (CENTA; grant reference NE/S007350/1) and the University of Leicester, YM was supported by the Jackson Foundation and European Research Council Advanced Investigator Grant, GEM-TRAIT (321131), YM, RME, and TR by NERC grant NE/P002218/1, and RME is supported by the NOMIS Foundation. SB, PJ, CM and DFRPB were supported by the UK Natural Environment Research Council (NE/K016253/1). Maliau Basin and Danum Valley Management Committees, Royal Society South East Asia Rainforest Research Partnership (SEARRP), Sabah Foundation, Benta Wawasan, the State Secretary, Sabah Chief Minister's Departments, Sabah Forestry Department, Sabah Biodiversity Council, and the Economic Planning Unit are acknowledged for their support and access to the sites in Sabah. Rostin Jantan, Rohid Kailoh, Suhaini Patik, Ampat Siliwong, Jeffry Amin, Ryan Gray, Johnny Larenus, Unding Jami, Noreen Majalap, Toby Marthews, Alexander Karolus, the Danum 50 ha plot team, Glen Reynolds, Edgar Turner, Laura Kruitbos, Lisa P. Bentley, Benjamin Blonder, Puikiat Hoo, Alexander Shenkin, Chun Xing Wong, Bernadus Bala Ola, Bill McDonald and MinSheng Khoo helped with the stem respiration and plant traits data collection and logistics. Kasia Ziemińska, Hedda Weitz and Jaime Buckingham provided laboratory support during the wood anatomy campaign.

Competing interests

None declared.

Author contributions

MBM wrote the paper with contributions from TR, SP, JCB, JK, YM, RME and DFRPB; MBM analysed the data; YM,

RME, YAT, DFRPB, RR, CM and PJ contributed new reagents/analytic tools; TR, SB, PJ, WHH, RC and MMP performed the research; and YM, TR, RME, YAT and DFRPB designed the research.

ORCID

Juan Carlos Berrio  <https://orcid.org/0000-0002-9198-9277>
 Sabine Both  <https://orcid.org/0000-0003-4437-5106>
 David F. R. P. Burslem  <https://orcid.org/0000-0001-6033-0990>
 Rudi Cruz  <https://orcid.org/0000-0003-1463-8278>
 Walter Huaraca Huasco  <https://orcid.org/0000-0001-5300-4986>
 Palasiah Jotan  <https://orcid.org/0000-0003-4973-9407>
 Jörg Kaduk  <https://orcid.org/0000-0003-4051-3081>
 Yadvinder Malhi  <https://orcid.org/0000-0002-3503-4783>
 Colin Maycock  <https://orcid.org/0000-0002-4368-2545>
 Maria B. Mills  <https://orcid.org/0000-0002-2902-8969>
 Susan Page  <https://orcid.org/0000-0002-3392-9241>
 Milenka M. Pillco  <https://orcid.org/0000-0002-5235-6899>
 Terhi Riutta  <https://orcid.org/0000-0002-8308-5307>
 Yit A. Teh  <https://orcid.org/0000-0001-7976-6794>

Data availability

Dataset of stem CO₂ efflux for individual trees is available at doi: [10.5281/zenodo.12799889](https://doi.org/10.5281/zenodo.12799889), plant functional traits for individual trees at doi: [10.5281/zenodo.3247631](https://doi.org/10.5281/zenodo.3247631) and community-weighted mean traits at doi: [10.5281/zenodo.3247602](https://doi.org/10.5281/zenodo.3247602), anatomical wood traits at doi: [10.5281/zenodo.5513918](https://doi.org/10.5281/zenodo.5513918), and stand-level carbon budget including stem respiration at doi: [10.5281/zenodo.7307449](https://doi.org/10.5281/zenodo.7307449).

References

- Amthor JS. 1989. Crop growth and maintenance respiration. *Respiration and Crop Productivity* 2: 69–104.
- Beer C, Reichstein M, Tomelleri E, Ciais P, Jung M, Carvalhais N, Rödenbeck C, Arain MA, Baldocchi D, Bonan GB *et al.* 2010. Terrestrial gross carbon dioxide uptake: global distribution and covariation with climate. *Science* 329: 834–838.
- Bischoff W, Newbery DM, Lingensfelder M, Schnaegel R, Petol GH, Madani L, Ridsdale CE. 2005. Secondary succession and dipterocarp recruitment in Bornean rain forest after logging. *Forest Ecology and Management* 218: 174–192.
- Both S, Riutta T, Paine CET, Elias DMO, Cruz RS, Jain A, Johnson D, Kritzler UH, Kuntz M, Majalap-Lee N *et al.* 2019. Logging and soil nutrients independently explain plant trait expression in tropical forests. *New Phytologist* 221: 1853–1865.
- Bowman WP, Turnbull MH, Tissue DT, Whitehead D, Griffin KL. 2008. Sapwood temperature gradients between lower stems and the crown do not influence estimates of stand-level stem CO₂ efflux. *Tree Physiology* 28: 1553–1559.
- Campbell G, Rabelo GR, Cunha MD. 2016. Ecological significance of wood anatomy of *Alseis pickelii* Pilg. & Schmale (Rubiaceae) in a tropical dry forest. *Acta Botânica Brasileira* 30: 124–130.
- Cavaleri MA, Oberbauer SF, Ryan MG. 2006. Wood CO₂ efflux in a primary tropical rain forest. *Global Change Biology* 12: 2442–2458.
- Chambers JQ, Higuchi N, Teixeira LM, Dos SJ, Laurance SG, Trumbore SE. 2004a. Response of tree biomass and wood litter to disturbance in a Central Amazon forest. *Oecologia* 141: 596–614.
- Chambers JQ, Tribuzy ES, Toledo LC, Crispim BF, Higuchi N, Santos JD, Araujo AC, Araujo A, Kruijt B, Nobre AD *et al.* 2004b. Respiration from a tropical forest ecosystem: partitioning of sources and low carbon use efficiency. *Ecological Applications* 14: 72–88.
- Chave J, Andalo C, Brown S, Cairns MA, Chambers JQ, Eamus D, Fölster H, Fromard F, Higuchi N, Kira T *et al.* 2005. Tree allometry and improved estimation of carbon stocks and balance in tropical forests. *Oecologia* 145: 87–99.
- Chen G, Yang Y, Robinson D. 2013. Allocation of gross primary production in forest ecosystems: allometric constraints and environmental responses. *New Phytologist* 200: 1176–1186.
- Cleveland CC, Reed SC, Townsend AR. 2006. Nutrient regulation of organic matter decomposition in a tropical rain forest. *Ecology* 87: 492–503.
- DeArmond D, Ferraz JBS, Marra DM, Amaral MRM, Lima AJN, Higuchi N. 2022. Logging intensity affects growth and lifespan trajectories for pioneer species in Central Amazonia. *Forest Ecology and Management* 522: 120450.
- Ewers RM, Didham RK, Fahrig L, Ferraz G, Hector A, Holt RD, Kapos V, Reynolds G, Sunin W, Snaddon JL *et al.* 2011. A large-scale forest fragmentation experiment: the stability of altered forest ecosystems project. *Philosophical Transactions of the Royal Society B: Biological Sciences* 366: 3292–3302.
- Figueira AM, Miller SD, De SCAD, Menton MC, Maia AR, Da RHR, Goulden ML. 2008. Effects of selective logging on tropical forest tree growth. *Journal of Geophysical Research: Biogeosciences* 113: 1–11.
- Fisher B, Edwards DP, Giam X, Wilcove DS. 2011. The high costs of conserving Southeast Asia's lowland rainforests. *Frontiers in Ecology and the Environment* 9: 329–334.
- Fromm J. 2010. Wood formation of trees in relation to potassium and calcium nutrition. *Tree Physiology* 30: 1140–1147.
- Han F, Wang X, Zhou H, Li Y, Hu D. 2017. Temporal dynamics and vertical variations in stem CO₂ efflux of *Styphnolobium japonicum*. *Journal of Plant Research* 130: 845–858.
- Harris NL, Hall CAS, Lugo AE. 2008. Estimates of species- and ecosystem-level respiration of woody stems along an elevational gradient in the Luquillo Mountains, Puerto Rico. *Ecological Modelling* 216: 253–264.
- Heineman KD, Turner BL, Dalling JW. 2016. Variation in wood nutrients along a tropical soil fertility gradient. *New Phytologist* 211: 440–454.
- Hölttä T, Kolari P. 2009. Interpretation of stem CO₂ efflux measurements. *Tree Physiology* 29: 1447–1456.
- Jardine KJ, Cobello LO, Teixeira LM, East MMS, Levine S, Gimenez BO, Robles E, Spanner G, Koven C, Xu C *et al.* 2022. Stem respiration and growth in a central Amazon rainforest. *Trees-Structure and Function* 36: 1–14.
- Jomo KS, Chang YT, Khoo KJ. 2004. *Deforesting Malaysia: the political economy and social ecology of agricultural expansion and commercial logging*. London, UK: Zed Books.
- Jotan P, Maycock CR, Burslem DF, Ahmad B. 2020. Comparative vessel traits of macaranga gigantea and vatica dulitensis from Malaysian Borneo. *Journal of Tropical Forest Science* 32: 25–34.
- Katayama A, Kume T, Ohashi M, Matsumoto K, Nakagawa M, Saito T, Kumagai T, Otsuki K. 2016. Characteristics of wood CO₂ efflux in a Bornean tropical rainforest. *Agricultural and Forest Meteorology* 220: 190–199.
- King DA, Davies SJ, Tan S, Noor NSM. 2006. The role of wood density and stem support costs in the growth and mortality of tropical trees. *Journal of Ecology* 94: 670–680.
- Köhler P, Ditzer T, Huth A. 2000. Concepts for the aggregation of tropical tree species into functional types and the application to Sabah's lowland rain forests. *Journal of Tropical Ecology* 16: 591–602.
- Kucheryavskiy S. 2020. MDATools – R package for chemometrics. *Chemometrics and Intelligent Laboratory Systems* 198: 103937.
- Kumagai T, Porporato A. 2012. Drought-induced mortality of a Bornean tropical rain forest amplified by climate change. *Journal of Geophysical Research: Biogeosciences* 117: 4–13.
- Kunert N, El-Madany TS, Aparecido LMT, Wolf S, Potvin C. 2019. Understanding the controls over forest carbon use efficiency on small spatial scales: effects of forest disturbance and tree diversity. *Agricultural and Forest Meteorology* 269–270: 136–144.
- Lanning M, Wang L, Scanlon TM, Vadeboncoeur MA, Adams MB, Epstein HE, Druckenbrod D. 2019. Intensified vegetation water use under acid deposition. *Science Advances* 5: eaav5168.

- Laurance WF, Sayer J, Cassman KG. 2014. Agricultural expansion and its impacts on tropical nature. *Trends in Ecology & Evolution* 29: 107–116.
- Li C-P, Qi Y-P, Zhang J, Yang L-T, Wang D-H, Ye X, Lai N-W, Tan L-L, Lin D, Chen L-S. 2017. Magnesium-deficiency-induced alterations of gas exchange, major metabolites and key enzymes differ among roots, and lower and upper leaves of *Citrus sinensis* seedlings. *Tree Physiology* 37: 1564–1581.
- Malhi Y. 2012. The productivity, metabolism and carbon cycle of tropical forest vegetation. *Journal of Ecology* 100: 65–75.
- Malhi Y, Aragão LEOC, Metcalfe DB, Paiva R, Quesada CA, Almeida S, Anderson L, Brando P, Chambers JQ, da Costa ACL *et al.* 2009. Comprehensive assessment of carbon productivity, allocation and storage in three Amazonian forests. *Global Change Biology* 15: 1255–1274.
- Malhi Y, Girardin C, Metcalfe DB, Doughty CE, Aragão LEOC, Rifai SW, Oliveras I, Shenkin A, Aguirre-Gutiérrez J, Dahlsjö CAL *et al.* 2021. The Global Ecosystems Monitoring network: monitoring ecosystem productivity and carbon cycling across the tropics. *Biological Conservation* 253: 108889.
- Mam Rasul G, Akram R, Esmail PDA. 2011. The role of magnesium in increasing of phosphorus fertilizer efficiency and wheat yield. *Mesopotamia Journal of Agriculture* 39: 33–39.
- Marthews T, Riutta T, Menor IO, Urrutia R, Moore S, Metcalfe D, Malhi Y, Phillips O, Huasco WH, Del Carmen M *et al.* 2014. *Measuring tropical forest carbon allocation and cycling: a RAINFOR-GEM field manual for intensive census plots (v.3.0) Manual*. Global Ecosystem Monitoring Network. [WWW document] URL <http://gem.tropicalforests.ox.ac.uk/> [accessed 9 August 2024].
- Meir P, Grace J. 2002. Scaling relationships for woody tissue respiration in two tropical rain forests. *Plant, Cell & Environment* 25: 963–973.
- Mills MB, Malhi Y, Ewers RM, Kho LK, Teh YA, Both S, Burslem DFRP, Majalap N, Nilus R, Huaraca Huasco W *et al.* 2023. Tropical forests post-logging are a persistent net carbon source to the atmosphere. *Proceedings of the National Academy of Sciences, USA* 120: e2214462120.
- Ogawa K. 2006. Stem respiration is influenced by pruning and girdling in *Pinus sylvestris*. *Scandinavian Journal of Forest Research* 21: 293–298.
- Ollech D. 2021. SEASTESTS: seasonality tests. R package v.0.15.4. [WWW document] URL <https://CRAN.R-project.org/package=seastests> [accessed 9 August 2024].
- Oulehle F, Urban O, Tahovská K, Kolář T, Rybníček M, Büntgen U, Hruška J, Čáslavský J, Trnka M. 2023. Calcium availability affects the intrinsic water-use efficiency of temperate forest trees. *Communications Earth & Environment* 4: 1–8.
- Pérez-Harguindeguy N, Díaz S, Garnier E, Lavorel S, Poorter H, Jaureguiberry P, Bret-Harte MS, Cornwell WK, Craine JM, Gurvich DE *et al.* 2013. New handbook for standardised measurement of plant functional traits worldwide. *Australian Journal of Botany* 61: 167–234.
- Pfeifer M, Lefebvre V, Turner E, Cusack J, Khoo M, Chey VK, Ewers RM, Peni M. 2015. Deadwood biomass: an underestimated carbon stock in degraded tropical forests? *Environmental Research Letters* 10: 1–11.
- Pinard R, Howlett B, Davidson D. 1996. Site conditions limit pioneer tree recruitment after logging of dipterocarp forests in Sabah, Malaysia. *Biotropica* 28: 2.
- Pinheiro J, Bates D, R Core Team. 2023. nlme: linear and nonlinear mixed effects models. R package v.3.1-165. [WWW document] URL <https://CRAN.R-project.org/package=nlme> [accessed 9 August 2024].
- Piovesan G, Biondi F. 2021. On tree longevity. *New Phytologist* 231: 1318–1337.
- Pruyn ML, Gartner BL, Harmon ME. 2002. Respiratory potential in sapwood of old versus young ponderosa pine trees in the Pacific Northwest. *Tree Physiology* 22: 105–116.
- Pruyn ML, Harmon ME, Gartner BL. 2003. Stem respiratory potential in six softwood and four hardwood tree species in the central cascades of Oregon. *Oecologia* 137: 10–21.
- Quesada CA, Lloyd J, Schwarz M, Patiño S, Baker TR, Czimczik C, Fyllas NM, Martinelli L, Nardoto GB, Schmerler J *et al.* 2010. Variations in chemical and physical properties of Amazon forest soils in relation to their genesis. *Biogeosciences* 7: 1515–1541.
- R Core Team. 2024. *R: a language and environment for statistical computing*. Vienna, Austria: R Foundation for Statistical Computing.
- Reynolds G, Payne J, Sinun W, Mosigil G, Walsh RPD. 2011. Changes in forest land use and management in Sabah, Malaysian Borneo, 1990–2010, with a focus on the Danum Valley region. *Philosophical Transactions of the Royal Society B: Biological Sciences* 366: 3168–3176.
- Riutta T, Kho LK, Teh YA, Ewers R, Majalap N, Malhi Y. 2021. Major and persistent shifts in below-ground carbon dynamics and soil respiration following logging in tropical forests. *Global Change Biology* 27: 1–16.
- Riutta T, Malhi Y, Kho LK, Marthews TR, Huaraca Huasco W, Khoo M, Tan S, Turner E, Reynolds G, Both S *et al.* 2018. Logging disturbance shifts net primary productivity and its allocation in Bornean tropical forests. *Global Change Biology* 24: 2913–2928.
- Robertson AL, Malhi Y, Farfán-Amezquita F, Aragão LEOC, Silva Espejo JE, Robertson MA. 2010. Stem respiration in tropical forests along an elevation gradient in the Amazon and Andes. *Global Change Biology* 16: 3193–3204.
- Rodionova OY, Pomerantsev AL. 2020. Detection of outliers in projection-based modeling. *Analytical Chemistry* 92: 2656–2664.
- Rodríguez-Calcerrada J, López R, Salomón R, Gordaliza GG, Valbuena-Carabaña M, Oleksyn J, Gil L. 2015. Stem CO₂ efflux in six co-occurring tree species: underlying factors and ecological implications. *Plant, Cell & Environment* 38: 1104–1115.
- Rogiers SY, Greer DH, Moroni FJ, Baby T. 2020. Potassium and magnesium mediate the light and CO₂ photosynthetic responses of grapevines. *Biology* 9: 1–18.
- Rowland L, da Costa ACL, Oliveira AAR, Oliveira RS, Bittencourt PL, Costa PB, Giles AL, Sosa AI, Coughlin I, Godlee JL *et al.* 2018. Drought stress and tree size determine stem CO₂ efflux in a tropical forest. *New Phytologist* 218: 1393–1405.
- Rowland L, Oliveira RS, Bittencourt PRL, Giles AL, Coughlin I, Costa PB, Domingues T, Ferreira LV, Vasconcelos SS, Junior JAS *et al.* 2021. Plant traits controlling growth change in response to a drier climate. *New Phytologist* 229: 1363–1374.
- Ryan MG, Binkley D, Fownes JH, Giardina CP, Senock RS. 2004. An experimental test of the causes of forest growth decline with stand age. *Ecological Monographs* 74: 393–414.
- Ryan MG, Cavaleri MA, Almeida AC, Penchel R, Senock RS, Luiz SJ. 2009. Wood CO₂ efflux and foliar respiration for Eucalyptus in Hawaii and Brazil. *Tree Physiology* 29: 1213–1222.
- Ryan MG, Phillips N, Bond BJ. 2006. The hydraulic limitation hypothesis revisited. *Plant, Cell & Environment* 29: 367–381.
- Salomón RL, Helm J, Gessler A, Grams TEE, Hilman B, Muhr J, Steppe K, Wittmann C, Hartmann H. 2024. The quandary of sources and sinks of CO₂ efflux in tree stems—new insights and future directions. *Tree Physiology* 44: tpad157.
- Saner P, Loh YY, Ong RC, Hector A. 2012. Carbon stocks and fluxes in tropical lowland dipterocarp rainforests in Sabah, Malaysian Borneo. *PLoS ONE* 7: 29642.
- Sitch S, Friedlingstein P, Gruber N, Jones SD, Murray-Tortarolo G, Ahlström A, Doney SC, Graven H, Heinze C, Huntingford C *et al.* 2015. Recent trends and drivers of regional sources and sinks of carbon dioxide. *Biogeosciences* 12: 653–679.
- Struebig MJ, Turner A, Giles E, Lasmana F, Tollington S, Bernard H, Bell D. 2013. Quantifying the biodiversity value of repeatedly logged rainforests: gradient and comparative approaches from Borneo. *Advances in Ecological Research* 48: 183–224.
- Teskey RO, Saveyn A, Steppe K, McGuire MA. 2008. Origin, fate and significance of CO₂ in tree stems. *New Phytologist* 177: 17–32.
- Trap J, Bureau F, Perez G, Aubert M. 2013. PLS-regressions highlight litter quality as the major predictor of humus form shift along forest maturation. *Soil Biology and Biochemistry* 57: 969–971.
- Trumbore SE, Angert A, Kunert N, Muhr J, Chambers JQ. 2013. What's the flux? Unraveling how CO₂ fluxes from trees reflect underlying physiological processes. *New Phytologist* 197: 353–355.
- Vitoria AP, Vieira TDO, Camargo PDB, Santiago LS. 2016. Using leaf δ¹³C and photosynthetic parameters to understand acclimation to irradiance and leaf age effects during tropical forest regeneration. *Forest Ecology and Management* 379: 50–60.

- Walsh RPD, Newbery DM. 1999. The ecoclimatology of Danum, Sabah, in the context of the world's rainforest regions, with particular reference to dry periods and their impact. *Philosophical Transactions of the Royal Society of London. Series B: Biological Sciences* 354: 1869–1883.
- Xu X, Sun Z, Hao Z, Bian Q, Wei K, Wang C. 2021. Effects of urban forest types and traits on soil organic carbon stock in Beijing. *Forests* 12: 394.
- Zach A, Horna V, Leuschner C. 2008. Elevational change in woody tissue CO₂ efflux in a tropical mountain rain forest in southern Ecuador. *Tree Physiology* 28: 67–74.
- Zach A, Horna V, Leuschner C, Zimmermann R. 2010. Patterns of wood carbon dioxide efflux across a 2000-m elevation transect in an Andean moist forest. *Oecologia* 162: 127–137.
- Zanne AE, Lopez-Gonzalez G, Coomes DA, Ilic J, Jansen S, Lewis SL, Miller RB, Swenson NG, Wiemann MC, Chave J. 2009. Data from: Towards a worldwide wood economics spectrum (Version 5) [Data set]. *Dryad*. doi: 10.5061/DRYAD.234.
- Zema DA, Parhizkar M, Plaza-Alvarez PA, Xu X, Lucas-Borja ME. 2023. Using random forest and multiple-regression models to predict changes in surface runoff and soil erosion after prescribed fire. *Modeling Earth Systems and Environment* 10: 1215–1228.

Supporting Information

Additional Supporting Information may be found online in the Supporting Information section at the end of the article.

Fig. S1 1-ha study plot species composition with species sampled.

Fig. S2 Diameter class structure and contribution of diameter classes to basal for each 1-ha study plot.

Fig. S3 Illustration and photographs of collar set-up for flux measurements.

Fig. S4 Linear model of basal area and surface area index with stand-level efflux, and maintenance respiration with surface area index.

Fig. S5 Principal component analysis scores for soil traits (0–10 cm) across 1-ha study plots.

Table S1 Description and short explanation of the plant functional traits, community-weighted means and soil variables used in this study.

Table S2 Output from the partial least squares regression models for logged and old-growth 1-ha study plots.

Please note: Wiley is not responsible for the content or functionality of any Supporting Information supplied by the authors. Any queries (other than missing material) should be directed to the *New Phytologist* Central Office.